Digital Object Identifier (DOI): 10.1109/IECON.2017.8216752

43rd Annual Conference of the IEEE Industrial Electronics Society

DC/DC conversion solutions to enable smart-grid behavior in the aircraft electrical power distribution system

Levy Ferreira Costa
Giampaolo Buticchi
Marco Liserre

Suggested Citation

G. Buticchi, L. Costa and M. Liserre, "DC/DC conversion solutions to enable smart-grid behavior in the aircraft electrical power distribution system," IECON 2017 - 43rd Annual Conference of the IEEE Industrial Electronics Society, Beijing, 2017, pp. 4369-4374.

DC/DC Conversion Solutions to enable Smart-grid Behavior in the Aircraft Electrical Power Distribution System

Giampaolo Buticchi
School of Science and Engineering
University of Nottingham Ningbo China
Email: buticchi@ieee.org

Levy Costa and Marco Liserre
Chair of Power Electronics
University of Kiel, Germany
Email: lfc,ml@tf.uni-kiel.de

***Abstract*—The more electric aircraft concept is pushing towards a DC distribution system for the on-board electrical appliances. In the scenario where multiple high-voltage and low-voltage buses are present, a power electronics converter interface is mandatory. In order to implement a resilient distribution system, the power exchange between different buses is envisaged, to ensure that a failure in a supply bus does not impair the rest of the distribution system.**

In this paper, two power converter structures able to achieve this goal are analyzed and compared in view of their contribution to improve the overall system resiliency. A control structure is investigated to manage the load supply with the desired priority. The variable virtual resistor control allows shifting the load priority on demand and, as a consequence, is found suitable for achieving the desired goals. Theoretical analysis and experiments are reported to prove the performance of the chosen solution, which is based on a QAB controlled with virtual resistors.

I. Introduction

Aircraft transportation is the enabler of the modern society's globalization and the backbone of mail and goods transportation. Eurostat [1] statistics show that the interest and the number of passengers is steadily growing year after year (4.4% from 2013 to 2014), and air freight and mail showed a 6.4% and 3.3% increase, respectively. In this framework, the reliability and the efficiency of the aircrafts is of paramount importance.

In a conventional aircraft, the fuel is burned to produce the propulsive power and a part of it powers the on-board systems. Gearboxes power a central hydraulic pump, that is used for the actuation system. Hydraulic actuators have the advantage of a high power density and simple control. However, the infrastructure composed of pipes is very bulky and a leakage impairs the hydraulic actuation and releases at the same time corrosive fluids. Unplanned maintenance due to a fault in the hydraulic system grounds the aircraft [2].

In order to reduce the weight, and consequently the fuel consumption, the idea to use more electric power on aircraft was proposed (More Electric Aircraft, MEA [3]). Indeed, the idea to eliminate the hydraulic systems from aircraft dates back to 30 years ago, but only recently the advancement of the technology in conjunction with the investments for the new aircrafts brought this topic in the spotlight.

The basic concept is that hydraulic actuators can be replaced by electromechanical actuators, thus eliminating the hydraulic distribution system. In order to power these actuators, the electric power must be generated and then distributed. A possibility is to have an electric machine connected to the turbine of the engine, so that a variable frequency three-phase system can be distributed [4]. A power converter performs the AC/AC conversion needed for the electric machine driving. While this solution allows removing the hydraulic power from the picture, the share of the electric power on the aircraft is greatly increased, making the electric power distribution system (EPDS) design a challenging task.

Since weight and fuel optimization are of key importance, a highly efficient and lightweight system is envisaged and an EPDS based on different voltage levels (high-voltage for high-power loads and low-voltage for the actuators) has attracted the interest of industry and academia. In fact, the standard MIL-STD-704F describes a multi-bus transmission system (Figure 1), where a high voltage bus at 270V is used to transmit the power, and a low-voltage 28V distribution feeds the loads. With these premises, DC/DC converters represent the enabler for this scenario [5].

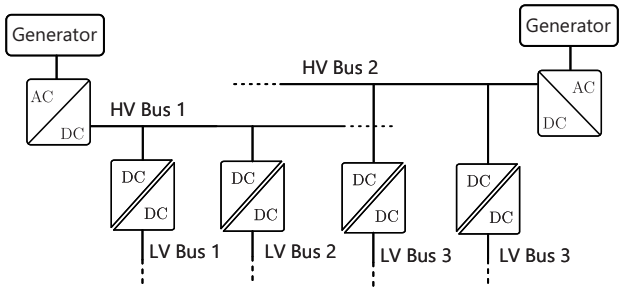

Fig. 1: Multi-bus architecture of More Electric Aircraft grid.

High resiliency is an important feature for the EPDS, since it is expected that the system still retains the functionality even in the case of faults in one or more parts. The fundamental issue of a system as described in Fig. 1 is that all the equipment connected to one bus ceases to function in the case of a fault

978-1-5386-1127-2/17/$31.00 ©2017 IEEE

on the bus or in the generator feeding that bus. This paper describes the possibility to realize the aircraft EPDS with a DC distribution system where power converter nodes manage the power exchange between different buses and the load priority. The possibility to route the power between the different HV and LV buses is a feature that allows increasing the resiliency of the system. A de-centralized control is proposed, and its ability to operate properly in case of multiple bus disconnection and of changing load priority is demonstrated with simulations.

II. State of the art of isolated DC/DC converters

In applications where isolation between the input and output voltage is required, with reduced losses and high power density, the isolated high frequency (HF) DC/DC converters are the best choice. Regardless the topology, the isolated converter is composed of a high frequency bridge, used to generate an HF AC waveform, a transformer and a rectifier (unidirectional or bidirectional), used to convert the AC voltage on the transformer secondary side into a DC voltage.

Among the topologies proposed in literature, of particular interest are the Full-Bridge DC/DC converter (FBC), that implements a phase-shift modulation to achieve zero-voltage-switching during the commutations. To further reduce the switching losses, full-resonant solutions were proposed, like the Series Resonant Converter (SRC) [6]: by adding a capacitor in series to the stray inductance of the transformer, ZCS commutation can be achieved. However, the fine control of the output voltage and current is difficult to achieve.

In applications like smart grid aerospace systems, where multiple loads and/or sources should be interconnected, multiple DC/DC converters are conventionally used. However, to avoid the use of several converters and the necessity of communication and synchronization among them, a centralized solution based on multi-port converter could be adopted. This would allow for a simpler control and the ability to exchange power among all ports. In particular, a multiple port converter based on multiple active bridges was proposed in 2007 in [7], [8] as a solution to interface a fuel cell generator, a battery storage system and passive loads. This converter is an extension of the Dual-Active-Bridge converter and it has three active bridges connected to the same high frequency multi-winding transformer. Because of its characteristics to have three active bridges, it was named as Triple-Active-Bridge converter (TAB). In [9] the TAB was extended to the aerospace EPDS to interface multiple HV buses.

Similarly, an extended version with four active bridges, called Quad-Active-Bridge (QAB, Fig. 2) was proposed in [10] to integrate distributed generation system and storage system to a solid-state transformer.

These solutions have the same characteristics and advantages of the DAB converter, with the additional advantage to integrate several power sources or loads with the minimum DC/DC conversion stages, implying a higher power density. Besides that, the power flow on the converter is easily controlled by using the phase-shift angle among the active bridges.

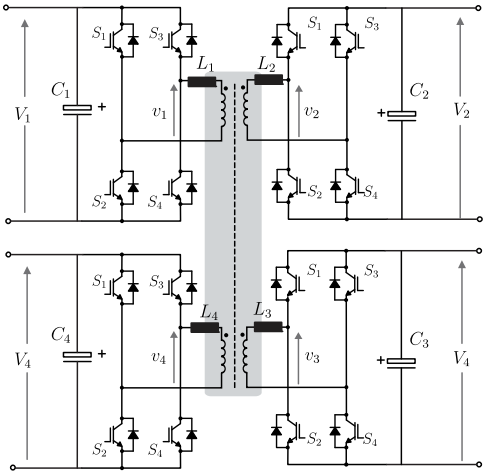

Fig. 2: Architecture of the Quadruple Active Bridge.

For these reasons, the multiple-active-bridge converter is a good choice to be used as a power manager device.

III. Multi-port based electrical distribution

The working hypothesis is to have a HV bus at 270 V for each generator, so that a minimum of two HV buses are present. In the LV side, at least two buses are present, one with the critical equipment and the other with loads that can be shed upon demand. The core of this paper is to upgrade the single-input single output-units in Fig. 1 with a multiple-input multiple-output units that enable the power transfer between multiple ports, like Fig. 3.

The easiest solution to realize a four port unit is to adopt a 2-DAB solution (Fig. 4a), however this topology does not comply with the resiliency requirement: in the case of a fault in a HV bus, a whole DAB unit is rendered useless. The QAB solution ((Fig. 4b) [11] has the same component count of the 2-DAB solution and the magnetic coupling allows the power exchange. Fig. 4c shows the possibility of employing a 3-DAB topology [12] to enable a resilient electrical distribution with 2-port power converters. However, the component count is 50% higher, since two H-bridge and an additional HF transformer are needed.

In Fig. 4 are also highlighted the possible power paths. Of particular interest is the power transfer from HV bus 1 to LV bus 2, that can be required in the case of a disconnection of HV bus 2. Solution a does not allow this operation, solution b guarantees the power transfer through 2 H-bridge and one HF transformer and solution c allows it through 6 H-bridges and three HF transformers. Solution b and c will be analyzed in the following.

The phase-shift control is adopted for QAB and DAB, that implies that each full-bridge is driven with a 50% duty cycle and the shifting between the voltage square waves determines the power transfer. Equation (1) and (2) describe the power transfer between a HV and a LV port. V^{HV} is the generic voltage at the HV bus, L_{lki} is the overall leakage inductance

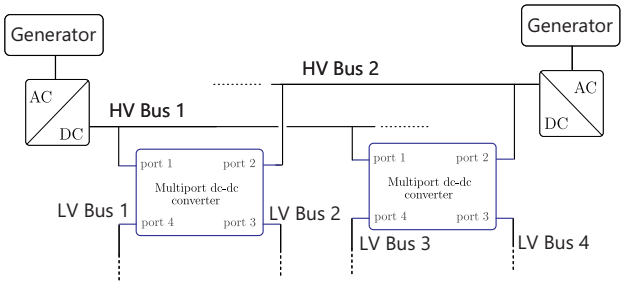

Fig. 3: Multi-bus architecture with the use of multi-port power converters.

seen from the two ports, f_{sw} is the frequency of the square-wave voltage excitation, and d_i is the phase shift normalized to 2π. It is important to note, that the leakage inductance to be used in (1) differs from the one in (2), because in the case of the QAB all ports participate in the power transfer.

$$i_{DC}^{LV} = \sum_i \frac{V_i}{L_{lki} f_{sw}} d_i \left(1 - 2d_i\right) \tag{1}$$

$$i_{DC}^{DAB} = \frac{V^{HV}}{L_{lk} f_{sw}} d \left(1 - 2d\right) \tag{2}$$

The control priority is to regulate the LV bus 1 at the reference voltage ($V_{LV}^{*} = 28V$). In order to do this, it is initially assumed that equal power is transferred from the two HV buses to LV bus 1.

IV. Virtual Resistor based control of the electrical distribution

In order to distribute the load priorities, virtual resistors [13] are used. The same approach was adopted in [9] and is here extended with different control targets for the QAB. The idea behind it is that a voltage control with a virtual resistor can be ideally represented by a voltage source with a series resistance. Increasing dynamically the resistance allows varying the output impedance of the voltage source, lowering the output voltage. This leads to a reduction of the current absorption for constant impedance loads, and can be used to perform load-shedding of a bus in the case of limited supply.The control structure is shown in Fig. 5.

The on-line change of the virtual resistor allows prioritizing some loads during different flight phases, paving the way for a re-configurable EPDS, that can still operate in a de-centralized way.

In the following, the mathematical model of the control is derived, in order to evaluate the two solutions and to give tuning guidelines. During normal operation, the voltage at the HV buses is assumed to be controlled, particular interest is the condition of the fault of HV bus 2, when the balancing regulators are operating. This situation is the most challenging from the stability point of view, because all three controllers interact with each other and it is assumed that the control is not changed after the fault occurrence.

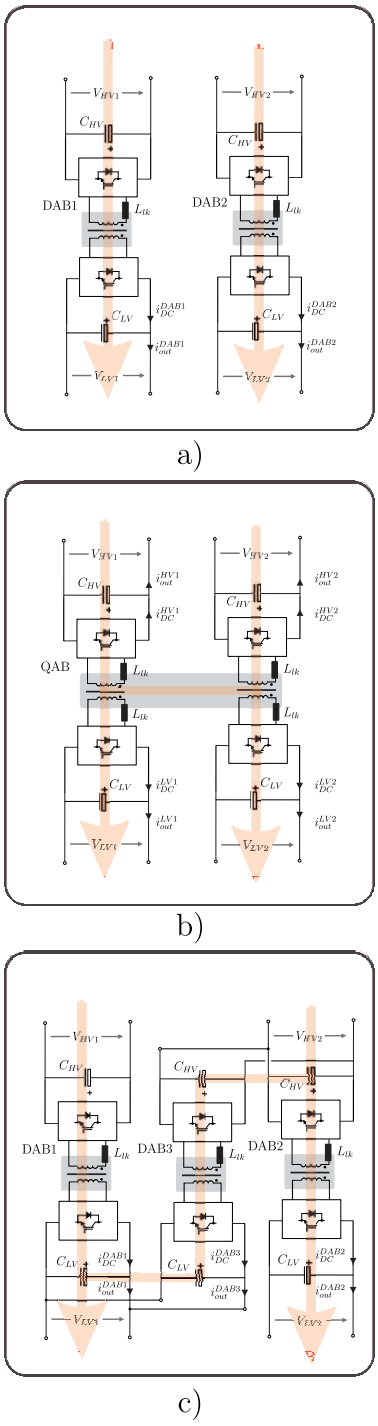

Fig. 4: Topology of the multi-port unit: a) 2-DAB converter b) QAB converter c) 3-DAB converter .

Equations (3)-(5) in Appendix I describe the capacitor voltage balance for the QAB solution, at this stage the QAB is modeled as three independent current source, each of them is directly proportional to the output of the PI regulators (as in Fig. 5), equations (6)-(8). This simplifications neglects the cross-coupling between different ports and the non-linearity of the phase-shift vs power transfer characteristic. It is worth

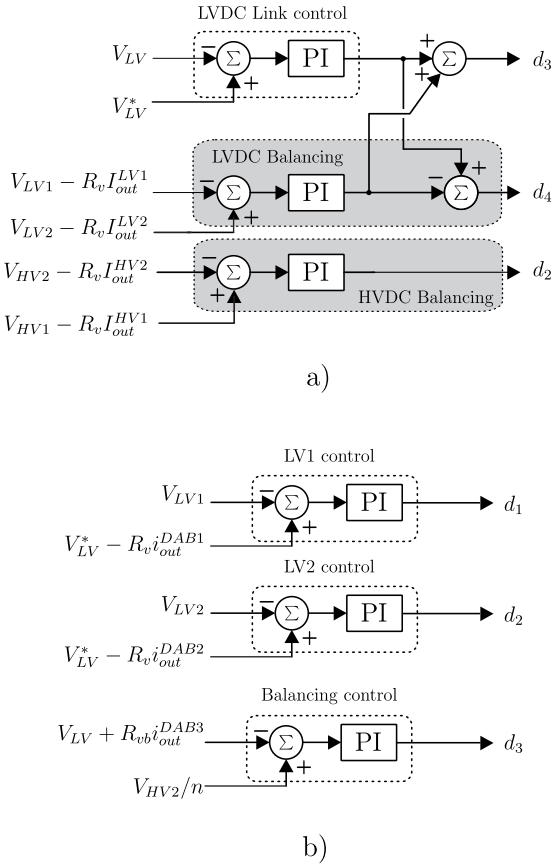

Fig. 5: Control of the QAB (a) and DABs (b) solutions.

mentioning that the particular structure of the control, where the output of the regulator is summed in one port and subtracted to the other allows for a partial compensation of the cross coupling effect.

The regulators are tuned with the symmetrical optimum criterion to have a crossover frequency of 100 Hz, the choice of the parameter is realized to have the same bandwidth for all loops. In the following it is assumed that the regulators directly control the current, as a consequence, a coefficient to compensate for this effect must be inserted in the actual control scheme. This coefficient represents the proportionality between the phase shift and the current and can be obtained by the derivative of the power equation (1), considering the nominal values for the DC bus. Due to the transformation ratio (that is chosen equal to the DC voltage ratio), the coefficient for the HV voltage balancing is $1/n$ times smaller than the one for the LV control and the LV balancing. Considering that also the HV and LV capacitance are chosen so that their ratio is the square of the voltage ratio, the actual parameters of the PI regulators can be determined.

The same procedure can be derived for the DAB structure (capacitor voltages in equations (9)-(11), PI regulators in (12)-(14). In this case, the control is slightly simpler, because each regulator has fewer inputs and no cross-coupling compensation is needed.

In a similar way of [13], the state-space model can be derived and the roots of the characteristic polynom represents the poles of the closed-loop transfer function. Same parameters were used for both topologies and are listed in TABLE I.

f_{sw}	20 kHz s	T_s	1e-4 s
L_{lk}	0.160 mH	I_{LV}	5 A
C_{HV}	0.01 mF	C_{LV}	1 mF

TABLE I: Simulation parameters.

The corresponding pole-zero map is shown in Fig. 6, showing complex conjugated poles for the DAB solution, but highlighting how the symmetrical optimum criterion in conjunction with the chosen control structure allows obtaining a stable system. The QAB solution, instead, shows only real poles.

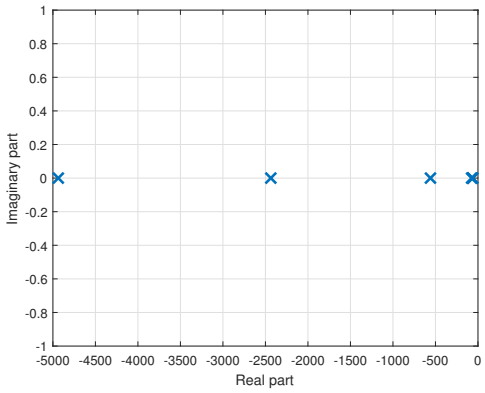

(a) QAB.

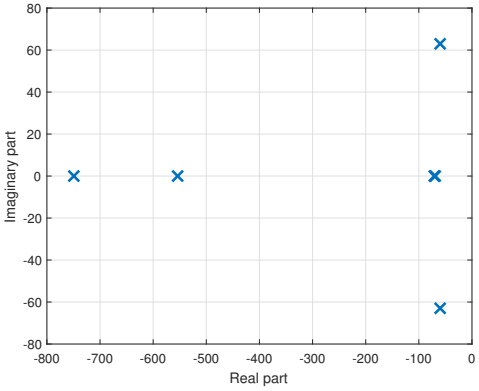

(b) DAB.

Fig. 6: Root locus for the two different units.

In order to prove that the state-space models is a good representation of the system, despite the many simplifications, its output is compared to a complete PLECS simulation (taking into account the high-frequency switching and the stray parameters of the circuit) in response of a load variation (5 A) at bus LV1 at t = 0.2 s and at HV2 (of 0.5 A) at t = 0.4 s. The results are shown in Fig. 7; for the state-space model of the QAB also the cross-coupling is considered. The duration of

the transient for the two solution is similar, but the QAB does not present overshoot. There is also a little mismatch for the DAB solution, because the voltage variation at the HV2 port also affects the power transfer to LV2 port. In the state-space model, this is not considered, and the voltage at LV2 remains constant.

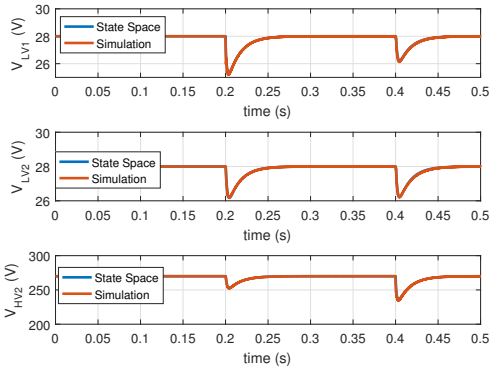

(a) QAB.

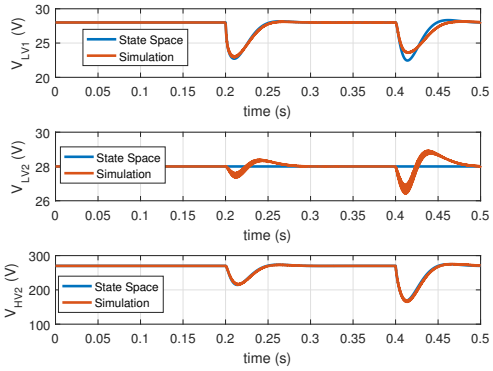

(b) DAB.

Fig. 7: Comparison between state-space and PLECS models in response to load variations.

V. Laboratory Results

The previous sections showed that the solutions based on DAB and QAB achieve a resilient behavior with similar dynamic performance. Due to the reduced component count and the shorter path between the ports ensured by the QAB solution, only this will be developed in laboratory. A symmetrical QAB prototype ($n = 1$) with 750 W power was used for preliminary testing to proof the virtual resistor concept. Port 1 and 2 are connected to two power supplies at 270 V and Port 3 and Port 4 are connected to electronic loads. Given that for the realized prototype all ports are at HV voltage, the subscripts LV and HV are not used in the results description, instead, V_1, V_2, V_3, V_4 and i^1_{out}, i^2_{out}, i^3_{out}, i^4_{out} are used to represent the DC voltages and DC output currents at each port. Figure 8 shows a picture of the laboratory setup. The control is the one described in Fig. 5. The series inductance for each port was $L_{lk} = 160\mu H$.

Fig. 9 shows a dynamic change of the virtual resistors, and the resistance of port 1 is changed from 3Ω to 9Ω. As can be seen, the currents are re-distributed with little impact on the voltage of Port 3. Also the high-frequency steady-state waveforms are reported.

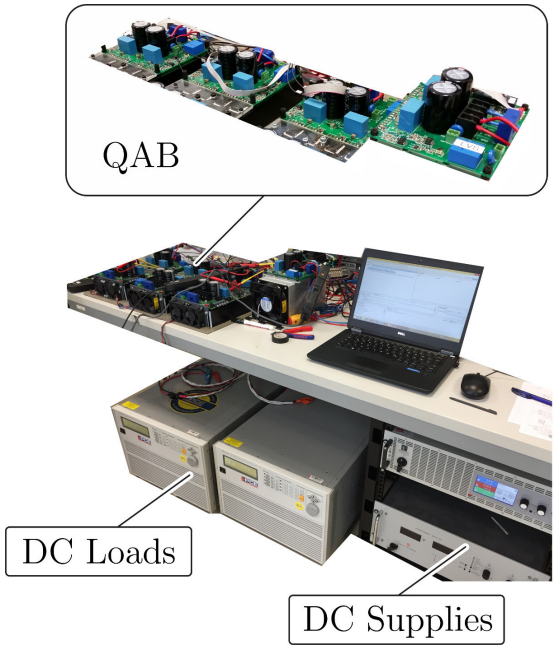

Fig. 8: Picture of experimental setup with the QAB prototype.

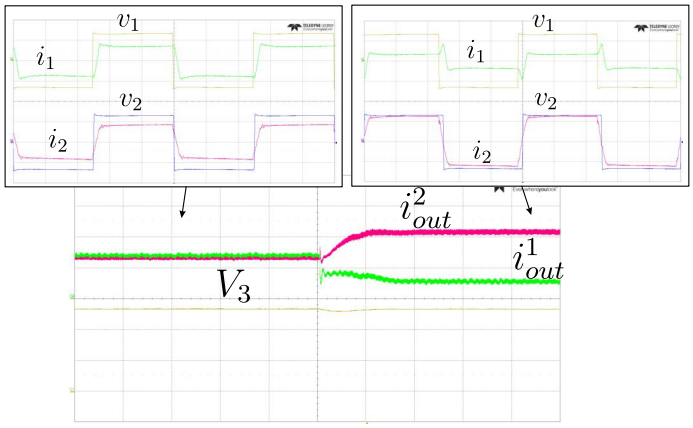

Fig. 9: Experiments: change of the virtual resistor for HV ports. v_1, v_2 200 V/div, i_1, i_2 2 A/div, time base 10 us/div. V_3 100 V/div, i^1_{out}, i^2_{out} 1 A/div, time base 50ms/div.

VI. Conclusion

This paper presents two solutions to implement multi-port DC/DC converter units for the electrical power distribution of a more electric aircraft. The main advantage with respect to the state of the art is that power transfer between different HV and LV buses is enabled. A virtual resistor based

control allows changing the priorities of the bus, enabling smart-grid operations. The solution based on a monolithic quadruple active bridge simplifies the design and reduces the total number of high-frequency transformers (1 HF transformer and 4 H-Bridges), however is sensitive to single-point failure. The solution based on DAB is more flexible and resilient to failures in the control, however it presents an increased component count (3 HF transformer and 6 H-bridges). State-space model and controls are described and simulation results shows the effectiveness of the two solutions during load steps. A prototype of the QAB converter embedding the proposed control has been realized, showing that the dynamic change of the virtual resistors allows redistributing the power between the ports.

APPENDIX I

QAB-based system.

$$V_{LV1} = \frac{1}{C_{LV}} \int i_{DC}^{LV1} dt \tag{3}$$

$$V_{LV2} = \frac{1}{C_{LV}} \int i_{DC}^{LV2} dt \tag{4}$$

$$V_{HV2} = \frac{1}{n\,(C_{HV})} \int i_{DC}^{HV2} dt \tag{5}$$

$$\begin{aligned} i_{DC}^{LV1} = {} & K_P^{LV} \left(V_{LV}^* - V_{LV1}\right) + K_I^{LV} \int \left(V_{LV}^* - V_{LV1}\right) dt + \\ & + K_P^{bLV} \left(V_{LV2} - R_v i_{out}^{LV2} - V_{LV1} + R_v i_{out}^{LV1}\right) + \\ & + K_I^{bLV} \int \left(V_{LV2} - R_v i_{out}^{LV2} - V_{LV1} + R_v i_{out}^{LV1}\right) dt + \\ & - \frac{K_P^{bHV}}{n} \left(V_{HV1} - R_v i_{out}^{HV1} - V_{HV2} + R_v i_{out}^{HV2}\right) + \\ & - \frac{K_I^{bHV}}{n} \int \left(V_{HV1} - R_v i_{out}^{HV1} - V_{HV2} + R_v i_{out}^{HV2}\right) dt \end{aligned} \tag{6}$$

$$\begin{aligned} i_{DC}^{LV2} = {} & K_P^{LV} \left(V_{LV}^* - V_{LV1}\right) + K_I^{LV} \int \left(V_{LV}^* - V_{LV1}\right) dt + \\ & - K_P^{bLV} \left(V_{LV2} - R_v i_{out}^{LV2} - V_{LV1} + R_v i_{out}^{LV1}\right) + \\ & - K_I^{bLV} \int \left(V_{LV2} - R_v i_{out}^{LV2} - V_{LV1} + R_v i_{out}^{LV1}\right) dt + \\ & - \frac{K_P^{bHV}}{n} \left(V_{HV1} - R_v i_{out}^{HV1} - V_{HV2} + R_v i_{out}^{HV2}\right) + \\ & - \frac{K_I^{bHV}}{n} \int \left(V_{HV1} - R_v i_{out}^{HV1} - V_{HV2} + R_v i_{out}^{HV2}\right) dt \end{aligned} \tag{7}$$

$$\begin{aligned} i_{DC}^{HV2} = {} & K_P^{bHV} \left(V_{HV1} - R_v i_{out}^{HV1} - V_{HV2} + R_v i_{out}^{HV2}\right) + \\ & K_I^{bHV} \int \left(V_{HV1} - R_v i_{out}^{HV1} - V_{HV2} + R_v i_{out}^{HV2}\right) dt \end{aligned} \tag{8}$$

DAB-based system.

$$V_{LV1} = \frac{1}{2C_{LV}} \int \left(i_{DC}^{DAB1} + i_{DC}^{DAB3}\right) dt \tag{9}$$

$$V_{LV2} = \frac{1}{C_{LV}} \int \left(i_{DC}^{DAB2}\right) dt \tag{10}$$

$$V_{HV2} = \frac{1}{n\,(2C_{HV})} \int -\left(i_{DC}^{DAB2} + i_{DC}^{DAB3}\right) dt \tag{11}$$

$$\begin{aligned} i_{DC}^{DAB1} = {} & K_P^{LV} \left(V_{LV}^* - V_{LV1} + R_v i_{out}^{DAB1}\right) + \\ & + K_I^{LV} \int \left(V_{LV}^* - V_{LV1} + R_v i_{out}^{DAB1}\right) dt \end{aligned} \tag{12}$$

$$\begin{aligned} i_{DC}^{DAB2} = {} & K_P^{LV} \left(V_{LV}^* - V_{LV2} + R_v i_{out}^{DAB2}\right) + \\ & + K_I^{LV} \int \left(V_{LV}^* - V_{LV2} + R_v i_{out}^{DAB2}\right) dt \end{aligned} \tag{13}$$

$$\begin{aligned} i_{DC}^{DAB3} = {} & K_P^{bal} \left(V_{HV2}/n - V_{LV1} + R_{vb} i_{out}^{DAB3}\right) + \\ & + K_I^{bal} \int \left(V_{HV2}/n - V_{LV1} + R_{vb} i_{out}^{DAB3}\right) dt \end{aligned} \tag{14}$$

REFERENCES

[1] Eurostat. (2015) Air transport statistics.

[2] J. A. Rosero, J. A. Ortega, E. Aldabas, and L. Romeral, "Moving towards a more electric aircraft," *IEEE Aerospace and Electronic Systems Magazine*, vol. 22, no. 3, pp. 3–9, March 2007.

[3] P. W. Wheeler, J. C. Clare, A. Trentin, and S. Bozhko, "An overview of the more electrical aircraft," *Proceedings of the Institution of Mechanical Engineers, Part G: Journal of Aerospace Engineering*, vol. 227, no. 4, pp. 578–585, 2013.

[4] J. Chang, C. LeMond, and A. Wang, "Distributed system and methodology of electrical power regulation, conditioning and distribution on an aircraft," Aug. 17 2004, uS Patent 6,778,414.

[5] G. Buticchi, L. F. Costa, and M. Liserre, "Improving system efficiency for the more electric aircraft,a look at dc/dc converters for the avionic on-board dc microgrid," *IEEE Industrial Electronics Magazine*, vol. 11, no. 3, Sept 2017.

[6] F. C. Schwarz, "A method of resonant current pulse modulation for power converters," *IEEE Transactions on Industrial Electronics and Control Instrumentation*, vol. IECI-17, no. 3, pp. 209–221, May 1970.

[7] H. Tao, A. Kotsopoulos, J. L. Duarte, and M. A. M. Hendrix, "Family of multiport bidirectional dc-dc converters," *IEE Proceedings - Electric Power Applications*, vol. 153, no. 3, pp. 451–458, May 2006.

[8] J. L. Duarte, M. Hendrix, and M. G. Simoes, "Three-port bidirectional converter for hybrid fuel cell systems," *IEEE Transactions on Power Electronics*, vol. 22, no. 2, pp. 480–487, March 2007.

[9] B. Karanayil, M. Ciobotaru, and V. G. Agelidis, "Power flow management of isolated multiport converter for more electric aircraft," *IEEE Transactions on Power Electronics*, vol. 32, no. 7, pp. 5850–5861, July 2017.

[10] S. Falcones, R. Ayyanar, and X. Mao, "A dc-dc multiport-converter-based solid-state transformer integrating distributed generation and storage," *IEEE Transactions on Power Electronics*, vol. 28, no. 5, pp. 2192–2203, May 2013.

[11] G. Buticchi, L. F. Costa, and M. Liserre, "Resilient multi-bus distribution in more electric aircraft by means of dual active bridges," in *ISIE 07 - The 26th IEEE International Symposium on Industrial Electronics*, Jun 2017.

[12] G. Buticchi, L. F. Costa, and M. Liserre, "A quadruple active bridge electrical power distribution system for the more electric aircraft," in *ISIE 07 - The 26th IEEE International Symposium on Industrial Electronics*, Jun 2017.

[13] G. Buticchi, M. Andresen, M. Wutti, and M. Liserre, "Lifetime based power routing of a quadruple active bridge dc/dc converter," *IEEE Transactions on Power Electronics*, 2017.